Published in final edited form as:
Dev Biol. 2008 December 1; 324(1): 131–138. doi:10.1016/j.ydbio.2008.09.012.

A Novel Activity of the Dickkopf-1 Amino-terminal Domain Promotes Axial and Heart Development Independently of Canonical Wnt Inhibition

Oksana Korol, **Ruchika W. Gupta**, and **Mark Mercola***

Abstract

The secreted Dickkopf-1 (Dkk1) protein mediates numerous cell fate decisions and morphogenetic processes. Its carboxyl terminal cysteine-rich region (termed C1) binds LRP5/6 and inhibits canonical Wnt signaling. Paradoxically, the isolated C1 domain of Dkk1 as well as Wnt antagonists that act by sequestering Wnts, such as Frz-B, WIF-1 and Crescent, are poor mimics of the inductive and patterning activities of Dkk1 critical for heart and axial development. To understand the basis for the unique properties of Dkk1, we investigated the function of its amino terminal cysteine-rich region (N1). N1 does not bind LRP or Kremen nor inhibit Wnt signaling and has had no known function. We show that it can synergize with BMP antagonism to induce prechordal and axial mesoderm when expressed as an independent protein in *Xenopus* embryos. Moreover, we show that it can function *in trans* to complement the activity of C1 protein to mediate two embryologic functions of Dkk1: induction of chordal and prechordal mesoderm and specification of heart tissue from non-cardiogenic mesoderm. Remarkably, N1 also synergizes with WIF-1 and Crescent, indicating that N1 signals independently of C1 and its interactions with LRP. Since cleavage of Dkk1 is not detected, these results define N1 as a novel signaling domain within the intact protein that is responsible for the potent effects of Dkk1 on the induction and patterning of the body axis and heart. We conclude that this new activity is also likely to synergize with canonical Wnt inhibitory in the numerous developmental and disease processes that involve Dkk1.

Keywords

Dkk1; axial patterning; heart induction; *Xenopus*

INTRODUCTION

Dkk1 is a potent inducer of heart development in non-cardiogenic mesoderm, as demonstrated by the formation of ectopic hearts in normally non-cardogenic ventroposterior marginal zone (VMZ) explants of *Xenopus* embryos (Foley and Mercola, 2005; Schneider and Mercola, 2001), in posterior lateral plate mesoderm of chick embryos (Marvin et al., 2001), and in embryonic stem cell (ESC) cultures (Naito et al., 2006). Other secreted Wnt

***Address for Correspondence:** Burnham Institute for Medical Research, 10901 N.Torrey Pines Road, La Jolla, CA 92037, Tel: 858-795-5242, Email: mmercola@burnham.org.

antagonists, such as Wnt inhibitory factor-1 (WIF-1), Crescent, or Frz-B, are generally less potent inducers, whereas intracellular inhibitors of canonical Wnt signaling, such as GSK3β or a dominant negative version of TCF3, initiate cardiogenesis but do not stimulate the formation of beating heart muscle (Foley et al., 2006; Marvin et al., 2001; Schneider and Mercola, 2001). Loss of Dkk1 function in early mouse embryos causes anencephaly (Mukhopadhyay et al., 2001) and over-expression studies using *Xenopus* and zebrafish embryos (Glinka et al., 1998; Kazanskaya, 2000; Shinya et al., 2000) have confirmed its ability to induce head and anterior structures. Secondary body axes induced by combination of BMP inhibition and Dkk1 expression typically have ectopic heads with normally-positioned bilateral eyes, whereas similar expression of Frz-B, dominant negative Wnt8, or Cerberus yields cyclopic heads (Kazanskaya, 2000), suggesting that important differences exist between these Wnt antagonists and Dkk1. Here we investigated whether the early developmental inductive and patterning properties of Dkk1 are due to a novel activity that is independent of Wnt-antagonism.

Dkk1 consists of conserved amino-terminal (N1) and carboxy-terminal (C1) cysteine-rich regions. Antagonism of canonical Wnt signaling occurs through binding of C1 to LRP5/6 proteins on the surface of the cell and subsequent disruption of the cell surface Wnt/LRP5/6/Frizzled signaling complex (reviewed in Niehrs, 2006). Other secreted Wnt antagonists, such as WIF-1, Crescent, and Frz-B, function by binding and sequestering secreted Wnt proteins. The signaling properties of Wnts and Wnt antagonists have been extensively characterized (reviewed in Logan and Nusse, 2004; Niehrs, 2006). One difference that has emerged between Dkk1 (and Dkk2 and 4) and other Wnt antagonists is that, by binding LRP5/6, Dkk1/2/4 could bias signaling toward the non-canonical Wnt planar cell polarity (PCP) pathway that involves Frizzled but not LRP receptors. Another, but not mutually exclusive, explanation for Dkk1's distinct activity is that the amino terminal cysteine-rich domain of Dkk1 (N1) might harbor a new activity that could complement the canonical Wnt antagonizing properties of C1 and trigger signaling that is required for the full patterning and morphogenetic effects of the intact protein. N1 lacks Wnt antagonizing activity (Brott and Sokol, 2002) and no known signaling or biological function has been ascribed to this domain.

We found that the early embryological activity of Dkk1 indeed requires a novel activity that resides within the N1 domain. Deletion of the N1 domain impaired development of axial mesoderm, yet, when expressed as independent proteins, N1 synergized with C1 and other Wnt antagonists to promote development of chordal and prechordal mesoderm. N1 also synergized robustly with C1 and other Wnt antagonists to induce ectopic heart formation in non-cardiogenic mesoderm. These studies demonstrate that Dkk1 is a dual-function protein and that the C1 and N1 domains activate distinct signaling pathways. Since Dkk1 is not normally cleaved to yield independent amino- and carboxyl-terminal domains, we propose that Wnt inhibition and the novel N1 activity are needed in the intact protein for the normal induction of the heart and anterior structures.

MATERIALS AND METHODS

Xenopus embryology, explant culture and histology

Embryos were fertilized in vitro, dejellied in 2% cysteine–HCl, pH7.8, and maintained in 0.1x MMR (Peng, 1991) Embryos were staged according to Nieuwkoop and Faber (Nieuwkoop and Faber, 1994). Dorsoanterior marginal zone (DMZ) or ventroposterior marginal zone (VMZ) explants were dissected at stage 10.25–10.5, when the blastopore was clearly discernible. DMZ explants span the dorsoanterior 90° of the marginal zone to include the presumptive heart field and VMZ explants comprise the ventroposterior 60° (Schneider and Mercola, 2001). Dissections were performed in 0.75x MMR using a fine tungsten

needle and processed immediately or cultured in 0.75x MMR until sibling controls had reached appropriate stages. For animal cap explants (prospective ectoderm), tissue approximately 30° from the animal pole was dissected at stage 8 in 0.75x MMR.

Tissues were flash frozen for subsequent RNA isolation or fixed in MEMPFA (1M MOPS (pH 7.4), 20mM EGTA, and 10mM $MgSO_4$) for histological analyses. In situ hybridization was performed according the protocol of Harland (Harland, 1991). Digoxygenin-labelled probes were transcribed from the following linearized plasmid templates (restriction digest, polymerase): pCS2+-*Shh* (EcoRI, T3), pCS2+-*XNot* (HindIII, T3), pGEM-*XNkx2.5* (XbaI, T7), p*XαMHC* (HindIII, T7).

In some instances, explants after fixation as above were processed for whole mount immunostaining using the anti-cardiac Troponin-T (cTn-T) monoclonal antibody (CT3, Developmental Studies Hybridoma Bank, University of Iowa) and a Cy3-conjugated donkey anti-mouse secondary antibody (Jackson ImmunoResearch Laboratories).

Plasmids and mRNA for injections

mRNA was transcribed from pCS2-tBMPR, pCS2-DKK1, pCS2-Crescent, pCS2-WIF, pSP64T–Xwnt3a, pCS2BA-N1, and pCS2BA-C1 plasmids using SP6 mMessage mMachine kit (Ambion). pCS2BA-N1 and pCS2BA-C1 were constructed by moving previously described N1 and C1 sequences (Brott and Sokol, 2002) into an HA tag-containing pCS2 vector. All cDNAs used encode *Xenopus* proteins except those for Crescent (chick), Dkk1, C1 and N1 (all human). Injections were performed in 3% Ficoll in 1x MMR (Peng, 1991). For VMZ experiments, embryos were injected equatorially into the two ventral blastomeres at 4–8 cell stage. For animal cap experiments, embryos were injected into each blastomere at the 2-cell stage at the animal pole.

Quantification of explant data and data presentation

Explants were stripped of identifiers and scored blindly for phenotype (e.g. incidence of beating or marker expression). p-values were calculated by the Chi-square test.

Animal cap assays

Animal cap tissue (presumptive ectoderm) from injected (above) or uninjected embryos was dissected at stage 8 and allowed to heal. For gene induction, they were processed for Q-RT-PCR at stage 10. For cap elongation, Activin A (R&D Systems) in 0.75x MMR and 1 mg/ml BSA was added during healing and caps were photographed when sibling embryo controls reached stages 11 and 20.

Quantitative RT-PCR

10–12 explants were pooled from each round of injections and RNA was extracted using Qiagen RNeasy Lipid Tissue Kit (Qiagen). First strand synthesis was carried out using a poly-dT primer and Superscript II Reverse Transcriptase (Invitrogen). Real time RT-PCR was performed on a Roche Light Cycler using the Light Cycler FastStart DNA master SYBR Green I kit (Roche). Quantification was carried out by normalizing levels to amount of total cDNA using the ubiquitously expressed *EF1*α transcript. The *EF1*α primer spans an intron and PCR in the absence of RT thus confirmed that RNA samples were free from genomic DNA contamination. Experiments shown are representative of a minimum of three RT-PCR experiments were performed and each experiment included a minimum of three biological replicates. Inter-experimental data were normalized to positive control samples included in each experiment. Standard deviations of the combined data set were calculated as described (Dixon and Massey, 1983). Briefly, for an n-experiment set, the square of

standard deviation of the mean for the set equals the sum of squares of standard deviation for each experiment, divided by n^2. p-values were calculated by Student's T-test.

Primer Pairs were: *Chd* forward 5'-AAC TGC CAG GAC TGG ATG GT-3', reverse 5'-GGC AGG ATT TAG AGT TGC TTC-3' (Ta=62 °C) (Sasai et al., 1994); *Gsc* forward 5'-GCT GAT TCC ACC AGT GCC TCA CCA G-3', reverse 5'-GGT CCT GTG CCT CCT CTT CCT CCT G-3' (Ta=68 °C); *ADMP* forward 5-GAT GAT GGA AGG AGA GGA-3', reverse 5'-TCA TGT TCT GAC CCA AAG-3' (Ta=62 °C); *Vent1* forward 5'-TTC CCT TCA GCA TGG TTC AAC-3', reverse 5'-GCA TCT CCT TGG CAT ATT TGG-3' (Ta=58 °C) (Sander et al., 2007); *Vent2* forward 5'-GTT CTT TGG TGT GTA CGG-3', reverse 5'-GCA GGT AGA GCA TCT GAA-3' (Ta=58 °C) (Nitta et al., 2007); *EF1α* forward 5'-TAC CCT CCT CTT GGT CGT T-3', reverse 5'-GGT TTT CGC TGC TTT CTG-3' (Ta=58 °C) (Foley and Mercola, 2005), *Xpo* forward 5'-CCA CAG GTC CGA AGA G-3', reverse 5'-TCC AGC AGA GTG TCA T-3' (Ta=60 °C); *Xnr3* forward 5'-CGC TGG ACC TTG TTC TTT G-3', reverse 5'-GGG GGA TCA GGT TTA GCA T-3' (Ta=60 °C); *Tbx5* forward 5'-TAA GCA CCT ACA CGG C-3', reverse 5'- ACC CAA CTC CGA AGA C-3' (Ta=60 °C).

RESULTS

Novel Signaling Activity in the N-terminal domain of Dkk1

The dorsoanterior marginal zone (DMZ) of late blastula to early gastrula stage *Xenopus* embryos is characterized by low BMP and low canonical Wnt signaling. Inhibition of these signaling pathways by microinjection of synthetic mRNA encoding Dkk1 plus a truncated form of the BMP receptor (tBR) into the prospective ventroposterior marginal zone (VMZ) region of 4–8 cell embryos potently induces complete secondary body axes (e.g. Glinka et al., 1998; Kazanskaya, 2000).

mRNAs for microinjection (Fig. 1A) were prepared to encode isolated N1 and C1 domains, each with the native Dkk1 pro-region to produce secreted proteins (Methods). C1 in conjunction with tBR induced secondary axes (see below), consistent with C1's Wnt inhibitory activity in a sensitive and quantitative *Xsiamois* (*Xsia*) induction assay performed in animal caps (Fig. 1B). N1 lacked any detectable ability to antagonize Wnt3a (Fig. 1B). Moreover, N1 injection did not block Wnt3a–induced secondary body axes nor induce secondary body axes on its own (not shown), both in agreement with a previous report (Brott and Sokol, 2002). Thus, N1 retains little if any canonical Wnt antagonizing activity and lacks canonical Wnt signaling activity. Nonetheless, N1 showed a robust, dose-dependent induction of head and axial mesoderm in secondary body axes in the presence of tBR, as visualized by *Sonic hedgehog* (*Shh*) and *XNot* positive cells at neurula stages (stage 14–15). The secondary body axes were classified according to the anteriorwards extent and strength of *Shh* or *XNot* gene expression (Fig. 1D) and quantified by class. 80 pg of N1 mRNA yielded nearly maximal induction of *Shh* (n=27) and *XNot* (n=20), respectively, comparable to that achieved with similar amounts of C1, WIF-1, or Crescent (see below).

To clarify how N1 induced secondary head and axial mesoderm, we examined injected DMZ and VMZ tissues for changes in gene expression by quantitative real-time reverse transcription polymerase chain reaction (RT-PCR) as evidence of re-patterning by N1. In contrast, N1 plus tBR injected into the VMZ significantly increased expression of the dorsoanterior genes *Goosecoid* (*Gsc*), *Chordin* (*Chd*), and *anti-dorsalizing morphogenetic protein* (*ADMP*) over tBR alone (Fig. 2 right panels). These genes mark the early gastrula-stage (stage 10.5) DMZ (reviewed in De Robertis and Kuroda, 2004) and their elevated expression is consistent with induction of chordal and pre-chordal markers *XNot* and *Shh* in stage 14–15 embryos by N1 plus tBR (Fig. 1D,E). N1 alone, however, failed to induce these dorsoanterior genes. Expression of these genes reflects Nodal and Smad2 signaling (Cho et

al., 1991;Sander et al., 2007;Sasai et al., 1994); thus, together with the inability of N1 to induce ectopic axes when injected alone (not shown), we conclude that N1 alone is unlikely to activate the Nodal pathway. We corroborated this conclusion by showing that N1 alone did not induce cap elongation, which is a classical readout of mesoderm-induction, nor did it synergize with Activin A in this assay (Supplemental Fig. 1). N1 alone or in conjunction with tBR did not induce *Xenopus Nodal-related-3* (*Xnr3*) (Fig. 2, right bottom panel). N1 alone inhibited expression of ventroposterior markers *Vent1, Vent2* and *Xenopus-posterior* (*Xpo*) to an extent comparable to that of tBR alone (Fig. 2 left panels). Taken together, these results indicate that the N1 domain exerts a dorsoanteriorizing influence prior to the onset of gastrulation but does not appear to directly influence canonical Wnt or Nodal pathways.

Dkk1 N-terminal Domain Synergizes with Wnt Antagonists to Enhance Axial Development

We next investigated whether N1 could synergize with C1 when both were expressed as separate proteins. Complementarity *in trans* would be consistent with the model that the two domains are capable of signaling independently. As above, we scored secondary axes induced by N1 ± C1, WIF or Crescent in the presence of tBR. As shown in Fig. 1, N1 alone in this assay induced a diffuse and poorly organized pattern of *Shh*- and *XNot*-expressing tissue (Fig. 1D,E). C1 without N1 induced *Shh* expression at neurula stages (stages 14–15; Fig. 3A,B) in a dose-dependent manner. Despite apparent organization of *Shh* expression at neurula stages, C1-induced secondary axes examined at approximately stage 42 exhibited predominantly no eyes or cyclopia, at a dose of C1 (45 pg) selected to yield robust secondary body axes at high incidence (100%, n=14) (Fig. 3C,D). Intact Dkk1 (50 pg, 100% secondary body axes, n=15) typically had 2 eyes (Fig. 3C,D), supporting the view that the C1 protein is deficient relative to intact Dkk1 in stimulating developmental processes, such as migration of head mesoderm or induction of forebrain neurectoderm that normally split the single *Xenopus* eye field into two retinal primordia (Li et al., 1997).

Notably, escalating doses of N1 mRNA injected together with a constant submaximal dose of C1 (20 pg) resulted in a corresponding increase in the extent and quality of the secondary body axes marked by *Shh* (Fig. 3B). 20 pg (n=17) or 80 pg (n=18) of N1 mRNA directed nearly all of the secondary axes (red arrows, Fig. 3A) to exhibit the levels and anteriorwards extent of *Shh* expression seen in primary axes (black arrows, Fig. 3A) or Dkk1-induced secondary axes (Fig. 1D inset). Since N1 without C1 produced poorly organized secondary axes in this assay (Fig. 1 D, E), we conclude that N1 can complement C1 plus tBR *in trans*.

Axial induction by the secreted Wnt antagonists WIF-1 and Crescent was also potentiated by N1 (Fig. 3E–H). As with C1, 20 or 80 pg of N1 mRNA directed the Shh-expression pattern to match or exceed that in the primary axes (n=30 and 20 for WIF-1 and Crescent, respectively, for the 20 pg dose of N1; n=29 and 21 for WIF-1 and Crescent, respectively for the 80 pg dose of N1). Since WIF-1 and Crescent bind and sequester extracellular Wnt proteins rather than bind LRP5/6 and Kremen (for review see Niehrs, 2006), these results strongly indicate that the N1 domain within Dkk1 is unlikely to function solely by modulating the efficacy of C1, such as by enhancing binding of C1 to LRP5/6 and disrupting the Wnt/Frizzled/LRP5/6 signaling complex. Rather, these data support the model that N1 provides an independent signal that is integrated at another point in the signaling cascade, possibly at the level of intracellular signaling.

Interestingly, C1, Crescent and WIF-1 each induced a characteristic pattern of *Shh*-expressing chordomesodermal cells within the secondary body axes (compare Fig. 3A,E,G). Identical results were observed with *XNot* (not shown). The reason for the antagonist-specific patterns is unclear but probably reflects differing abilities to inhibit Wnt proteins present in the VMZ, including Wnts that signal through canonical β-catenin as well as non-canonical pathways, and differential patterning of head tissue (for instance, see Pera and De

Robertis, 2000; Wang et al., 1997). Notably, at these doses of Wnt antagonists, N1 did not alter the pattern of *Shh* expression, but potentiated the activity of the Wnt antagonist, providing further evidence that N1 acts via a distinct signaling pathway from C1, WIF-1 and Crescent and that the signals are integrated in order to specify secondary body axes.

Novel Heart-inducing Activity of the Dkk1 N-terminal Domain

Since the preceding experiments demonstrated that N1 is capable of complementing the activity of Wnt antagonists in the specification of body axes induced in conjunction with tBR, we tested whether N1 also complements Wnt antagonists in the formation of hearts and cement glands. As before, a constant dose of tBR and Crescent (Fig. 4A,C) or WIF-1 (Fig. 4B,D) mRNA was co-injected to induce a basal incidence of 30–40% heart induction visible by α*MHC* expression in a pattern similar to that of the native heart region in the primary body axes. N1 alone did not induce αMHC^+ heart tissue. In contrast, N1 robustly increased the frequency of αMHC^+ heart tissue in a dose-dependent manner, achieving ~90% induction with 80 pg of N1 mRNA (n=16 for the 80 pg dose of N1 and 20 pg of both Crescent and WIF-1, Fig. 4C,D).

In these embryos, N1 also increased the ability of WIF-1 plus tBR to induce the cement gland, which is considered the most anterior head structure in *Xenopus* embryos (Fig. 4B,E). Crescent plus tBR did not induce cement glands under these conditions (Fig. 4A). Just as N1 increased but did not qualitatively alter the *Shh* pattern induced by each Wnt antagonist, N1 combined with Crescent plus tBR also did not induce cement glands, despite an increase in heart formation (Fig. 4C). This reinforces the conclusion that N1 signals through a distinct pathway that is integrated with Wnt antagonism.

We next tested heart induction in a more direct assay that does not require tBR but instead evaluates the ability of a Wnt antagonist to directly respecify non-cardiogenic VMZ to form heart tissue (diagrammed in Fig. 5A). Dkk1 mRNA injected in prospective VMZ at the 4–16 cell stage potently re-specifies early gastrula-stage (stage 10–10.5) VMZ explants, so that they will form a cyst-like structure containing a rhythmically beating myocardial tube connected to residual endoderm when maintained in explant culture (Schneider and Mercola, 2001).

N1 alone did not induce ectopic hearts in the VMZ explant assay at any dose tested in numerous trials (up to 600 pg, Fig. 5B). 200 pg of C1 induced α*MHC* in VMZ explants but addition of increasing amounts of N1 robustly increased cardiomyogenic gene expression Fig. 5C). Similarly, escalating doses of N1 synergized with 340 pg of Crescent mRNA to induce α*MHC* (Fig. 5D). As an independent measure of induction, the incidence of explants that stained positively for cardiac troponin-T (cTn-T) was significantly increased by N1 plus Crescent relative to Crescent alone (Fig. 5E). However, the pattern of cTn-T immunostaining in N1 plus Crescent injected explants were small and isolated, characteristic of Crescent alone in contrast to the single heart tubes typically induced by intact Dkk1 (Fig. 5F).

DISCUSSION

Our results indicate that the amino terminal cysteine-rich region of Dkk1 elicits a novel signaling response that complements axial and heart inductive properties of canonical Wnt antagonists. Our data indicate that synergy between the signal transduction pathways activated by the N-and C-terminal regions contributes to the potency of Dkk1 in the induction of prechordal and chordal mesoderm as well as heart tissue. We did not detect any cleavage of the intact protein *in vivo* (not shown) nor are we aware of any reports of endogeous cleavage of Dkk1; thus, although the isolated N1 protein is functional, we favor

the model that the N- and C-terminal regions function in the context of the intact protein. We cannot rule out the possibility, however, that Dkk1 might be cleaved to release a functional N1 protein in certain normal or pathological conditions, and it is notable that cleavage of Dkk2 and Dkk4 into C-terminal and N-terminal domains has been reported in cell culture preparations (Krupnik et al., 1999).

Interestingly, although N1 robustly synergized with C1 as well as naturally occurring, secreted Wnt antagonists to induce axial and heart tissue, the qualitative pattern of *Shh* expression (Fig. 3A,E,G) or the pattern of cTn-T^+ myocardial tissue in VMZ explants (Fig. 5F) remained as induced by the elevated doses of each of the individual Wnt antagonists. These observations, coupled with the inability to block Wnt signaling (Fig. 1B) suggest that N1 and C1 bind to distinct receptors and that signaling is integrated distally, perhaps at the level of intracellular mediators. A potentially related issue is that although the heart-inducing potency of Dkk1 could be reconstituted by co-expression of N1 and Wnt antagonists (Fig. 5C–E), the typical heart morphogenesis apparent with Dkk1 was not reproduced by co-injection of N1 with Wnt antagonists (e.g. Crescent, Fig. 5F), suggesting that physically tethering the two activities protein might be biologically important.

Dkk1, 2 and 4 function by binding LRP5/6, thereby disrupting the canonical receptor-ligand signaling complex and also participates in the downregulation of Kremen proteins from the cell surface (Niehrs, 2006). Whether the N-terminal domains of other Dkk proteins also have similar or other activities is under investigation. Moreover, since LRP5/6 are required for canonical Wnt signaling, Dkk1, 2 and 4 differ from other Wnt antagonists by biasing the composition of Wnt receptors on the cell surface in favor of Frizzled receptors, which also initiate non-canonical signaling and this mechanism is likely to contribute to the observed stimulation of Jun kinase (JNK) activity by Dkk1 during development and disease (Caneparo, 2007; Lee, 2004; Pandur et al., 2002; Peng, 2006). Caneparo et al. recently reported that the heparin sulfate proteoglycan Kynpek synergizes with Dkk1 to activate JNK (Caneparo, 2007). It will be important to determine the specific receptor(s) for N1 and its intracellular mediators.

Finally, Dkk1 is involved in many natural embryological processes in addition to the early axial and heart development addressed in this paper, as well as in pathological settings as diverse as tumorigenesis (for example Qian et al., 2007; Voorzanger-Rousselot et al., 2007; Yamabuki et al., 2007) and rheumatoid arthritis (Diarra et al., 2007). It will be important to evaluate the influence that N1 might have in these settings, as well as in processes that have been examined experimentally using recombinant Dkk1 as a reagent to disrupt Wnt signaling.

Supplementary Material

Refer to Web version on PubMed Central for supplementary material.

Acknowledgments

MM gratefully acknowledges research support from the NHLBI (R37 HL059502, R33 HL88266), the California Institute for Regenerative Medicine (RC1-00132), and an exploratory pilot program and shared resources of the BIMR Cancer Center Support Grant (P30CA030199).

REFERENCES

Brott BK, Sokol SY. Regulation of Wnt/LRP signaling by distinct domains of Dickkopf proteins. Mol Cell Biol 2002;22:6100–6110. [PubMed: 12167704]

Caneparo L, Huang YL, Staudt N, Tada M, Ahrendt R, Kazanskaya O, Nierhrs C, Houart C. Dickkopf-1 regulates gastrulation movements by coordinated modulation of Wnt/betacatenin and Wnt/PCP activities, through interaction with the Dally-like homolog Knypek. Genes Dev 2007;21:465–480. [PubMed: 17322405]

Cho KWY, Blumberg B, Steinbeisser H, De Robertis EM. Molecular nature of Spemann's organizer: the role of the Xenopus homeobox gene goosecoid. Cell 1991;67:1111–1120. [PubMed: 1684739]

De Robertis EM, Kuroda H. Dorsal-Ventral Patterning and Neural Induction in Xenopus Embryos. Annu Rev Cell Dev Biol. 2004

Diarra D, Stolina M, Polzer K, Zwerina J, Ominsky MS, Dwyer D, Korb A, Smolen J, Hoffmann M, Scheinecker C, van der Heide D, Landewe R, Lacey D, Richards WG, Schett G. Dickkopf-1 is a master regulator of joint remodeling. Nat Med 2007;13:156–163. [PubMed: 17237793]

Dixon, WJ.; Massey, FJ. New York: McGraw-Hill Publishing Company; 1983. Introduction to Statistical Analysis.

Foley AC, Gupta RW, Guzzo RM, Korol O, Mercola M. Embryonic Heart Induction. Ann N Y Acad. Sci 2006;1080:85–96. [PubMed: 17132777]

Foley AC, Mercola M. Heart induction by Wnt antagonists depends on the homeodomain transcription factor Hex. Genes Dev 2005;19:387–396. [PubMed: 15687261]

Glinka A, Wu W, Delius H, Monaghan AP, Blumenstock C, Niehrs C. Dickkopf-1 is a member of a new family of secreted proteins and functions in head induction. Nature 1998;392:357–362. [PubMed: 9450748]

Harland, RM. In situ hybridization: an improved whole mount method for *Xenopus* embryos. In: Kay, BK.; Peng, HB., editors. Xenopus laevis: Practical uses in cell and molecular biology. Vol. Vol. 36. San Diego: Academic Press; 1991. p. 685-695.

Kazanskaya OG, Nierhrs AC. The role of Xenopus dickkopf1 in prechordal plate specification and neural patterning. Development 2000;127:4981–4992. [PubMed: 11044411]

Krupnik VE, Sharp JD, Jiang C, Robison K, Chickering TW, Amaravadi L, Brown DE, Guyot D, Mays G, Leiby K, Chang B, Duong T, Goodearl ADJ, Gearing DP, Sokol SY, McCarthy SA. Functional and structural diversity of the human Dickkopf gene family. Gene 1999;238:301–313. [PubMed: 10570958]

Lee A, He B, You L, Xu Z, Maziers J, Reguart N, Mikami I, Batra S, Jablons DM. Dickkopf-1 antagonizes Wnt signaling independent of beta-catenin in human mesothelioma. Biochem Biophys Comm 2004;323:1246–1250.

Li H, Tierney C, Wen L, Wu JY, Rao Y. A single morphogenetic field gives rise to two retina primordia under the influence of the prechordal plate. Development 1997;124:603–615. [PubMed: 9043075]

Logan CY, Nusse R. The Wnt signaling pathway in development and disease. Annu Rev Cell Dev Biol 2004;20:781–810. [PubMed: 15473860]

Marvin MJ, Di Rocco G, Gardiner A, Bush SM, Lassar AB. Inhibition of Wnt activity induces heart formation from posterior mesoderm. Genes Dev 2001;15:316–327. [PubMed: 11159912]

Mukhopadhyay M, Shtrom S, Rodriguez-Esteban C, Chen L, Tsukui T, Gomer L, Dorward DW, Glinka A, Grinberg A, Huang S-P, Niehrs C, Belmonte JCI, Westphal H. Dickkopf1 Is Required for Embryonic Head Induction and Limb Morphogenesis in the Mouse. Developmental Cell 2001;1:423–434. [PubMed: 11702953]

Naito AT, Shiojima I, Akazawa H, Hidaka K, Morisaki T, Kikuchi A, Komuro I. Developmental stage-specific biphasic roles of Wnt/beta-catenin signaling in cardiomyogenesis and hematopoiesis. Proc Natl Acad Sci U S A 2006;103:19812–19817. [PubMed: 17170140]

Niehrs C. Function and biological roles of the Dickkopf family of Wnt modulators. Oncogene 2006;25:7469–7481. [PubMed: 17143291]

Nieuwkoop, PD.; Faber, J. Normal table of Xenopus laevis (Daudin): a systematical and chronological survey of the development from the fertilized egg till the end of metamorphosis. New York: Garland Pub.; 1994.

Nitta KR, Takahashi S, Haramoto Y, Fukuda M, Tanegashima K, Onuma Y, Asashima M. The N-terminus zinc finger domain of Xenopus SIP1 is important for neural induction, but not for suppression of Xbra expression. Int. J. Dev. Biol 2007;51:321–325. [PubMed: 17554684]

Pandur P, Lasche M, Eisenberg LM, Kuhl M. Wnt-11 activation of a non-canonical Wnt signalling pathway is required for cardiogenesis. Nature 2002;418:636–641. [PubMed: 12167861]

Peng, HB. Solutions and Protocols. In: Kay, BK.; Peng, HB., editors. Xenopus laevis: Practical uses in cell and molecular biology. Vol. Vol. 36. San Diego: Academic Press; 1991. p. 657-662.

Peng SMC, Li J, Fan X, Cao Y, Duan E. Dickkopf-1 induced apoptosis in human placental choriocarcinoma is independent of canonical Wnt signaling. Biochem Biophys Comm 2006;350:641–647.

Pera EM, De Robertis EM. A direct screen for secreted proteins in Xenopus embryos identifies distinct activities for the Wnt antagonists Crescent and Frzb-1. Mech Dev 2000;96:183–195. [PubMed: 10960783]

Qian J, Xie J, Hong S, Yang J, Zhang L, Han X, Wang M, Zhan F, Shaughnessy JD Jr, Epstein J, Kwak LW, Yi Q. Dickkopf-1 (DKK1) is a widely expressed and potent tumor-associated antigen in multiple myeloma. Blood 2007;110:1587–1594. [PubMed: 17515399]

Sander V, Reversade B, De Robertis EM. The opposing homeobox genes Goosecoid and Vent1/2 self-regulate Xenopus patterning. EMBO Journal 2007;26:2955–2965. [PubMed: 17525737]

Sasai Y, Lu B, Steinbeisser H, Geissert D, Gont LK, De Robertis EM. Xenopus chordin: A novel dorsalizing factor activated by organizer-specific homeobox genes. Cell 1994;79:779–790. [PubMed: 8001117]

Schneider VA, Mercola M. Wnt antagonism initiates cardiogenesis in Xenopus laevis. Genes and Development 2001;15:304–315. [PubMed: 11159911]

Shinya M, Eschbach C, Clark M, Lehrach H, Furutani-Seiki M. Zebrafish Dkk1, induced by the pre-MBT Wnt signaling, is secreted from the prechordal plate and patterns the anterior neural plate. Mechanisms of Development 2000;98:3–17. [PubMed: 11044603]

Voorzanger-Rousselot N, Goehrig D, Journe F, Doriath V, Body JJ, Clezardin P, Garnero P. Increased Dickkopf-1 expression in breast cancer bone metastases. Br J Cancer 2007;97:964–970. [PubMed: 17876334]

Wang S, Krinks M, Moos M Jr. Frzb-1, an antagonist of Wnt-1 and Wnt-8, does not block signaling by Wnts −3A, −5A, or −11. Biochem Biophys Res Commun 1997;236:502–504. [PubMed: 9240469]

Yamabuki T, Takano A, Hayama S, Ishikawa N, Kato T, Miyamoto M, Ito T, Ito H, Miyagi Y, Nakayama H, Fujita M, Hosokawa M, Tsuchiya E, Kohno N, Kondo S, Nakamura Y, Daigo Y. Dikkopf-1 as a novel serologic and prognostic biomarker for lung and esophageal carcinomas. Cancer Res 2007;67:2517–2525. [PubMed: 17363569]

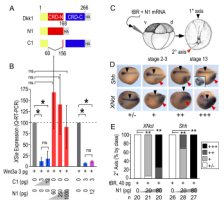

Figure 1. N1 lacks Wnt inhibitory activity but is active in secondary body axis induction

A) Fragments of Dkk1 expressed by microinjection in this study (see Methods).

B) *Xsia* induction by Wnt8 in animal cap tissue following injection of N1 and C1 assayed by quantitative real time RT-PCR. N1 has $<10^{-3}$-fold inhibitory activity relative to C1. Similar results were obtained for Wnt3a (activity $<10^{-2}$-fold relative to C1). Error bars indicate standard deviation (SD) and p values were calculated by Students T-test [*, <0.01; ns, not significant (>0.05)].

C) mRNAs were injected into the prospective VMZ region and embryos isolated at the neurula stage (stages 14–15).

D) *In situ* hybridization to *Shh* and *XNot* to visualize prechordal (*Shh*) and chordal (*Shh* and *XNot*) mesoderm in the primary (black arrows) and secondary body axes (red arrows) induced by N1 in conjunction with tBR. Class of secondary axes observed is indicated by: +/−, no or faint secondary axis; +, stronger staining but minimal anteriorwards extension; ++, strong staining, modest anteriorwards extension, and +++, robust staining and extensive anteriorwards extension. Note that secondary axis *Shh* and *XNot* staining was broader and appeared disorganized compared to the typically narrow pattern of the primary axis. For comparison, the inset shows an embryo with a secondary axis induced by Dkk1 plus tBR.

E) Quantification of the percentage of secondary axes induced according to class. p-values calculated by Chi-square test (**, <0.001). Representative of 2 trials with similar outcomes.

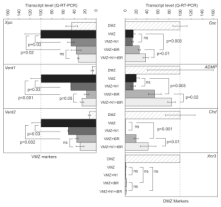

Figure 2. N1 alters dorsoventral pattern before gastrulation

VMZ explants were dissected from embryos at onset of gastrulation (stage 10) and analyzed for ventroposterior (left panels) or dorsoanterior (right panels) marker expression by quantitative real-time RT-PCR (Methods). Ventroposterior and dorsoanterior marker gene expression levels were normalized to uninjected VMZ or DMZ tissues, respectively. Experiments are the cumulative results of 3 independent experiments, each with at least 3 biological replicates. Error bars indicate SD and p-values were calculated by Student's T-test. Note that N1 alone reduces expression of *Xpo, Vent1* and *Vent2* indicating a dorsoanteriorizing effect but that induction of dorsoanterior markers *Gsc, Chd*, and *ADMP* occurs only in presence of tBR. *Xnr3* is not induced by N1 either alone or with tBR.

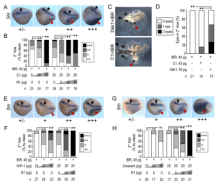

Figure 3. N1 complements C1 and secreted Wnt antagonists in trans

A,B) Complementation of axial induction by C1. Embryos were injected as described in Fig. 1 with N1, C1 and tBR mRNAs as indicated. *In situ* hybridization to *Shh* (A) revealed primary (black arrowheads) and secondary (red arrowheads) axes. The criteria used to score classes of secondary axes are shown (A) and indicated by +/−, +, ++, and +++. Dose-dependence of secondary axis induction in response to C1 plus tBR and N1, C1 plus tBR is shown according to class (B). The experiments using N1 and C1 are representative of 2 trials with similar outcomes; similar outcomes were also observed in additional experiments using 5 and 80 pg doses of C1. **C,D)** Examples of eye phenotype of secondary heads in embryos cultured until stage 45 (C). Quantification of eye number in secondary axes of embryos injected with tBR, tBR and C1, and tBR and Dkk1 (D).

E–H) Complementation of axial induction by WIF-1 (E,F) and Crescent (G,H) as in panels A,B. Note that complementation by N1 increases strength of axial induction but retains characteristic pattern of induced *Shh* expressing axial mesoderm. Thus, the criteria used to score secondary axes were stereotypical for each inducer (E,G). Results showing complementarity are for 20 pg of Crescent and WIF-1; similar outcomes were observed in additional experiments using 5 and 80 pg doses of Crescent and WIF-1.

p-values were calculated by the Chi-square test [**, <0.001; *, <0.05; ns, not significant (>0.05)].

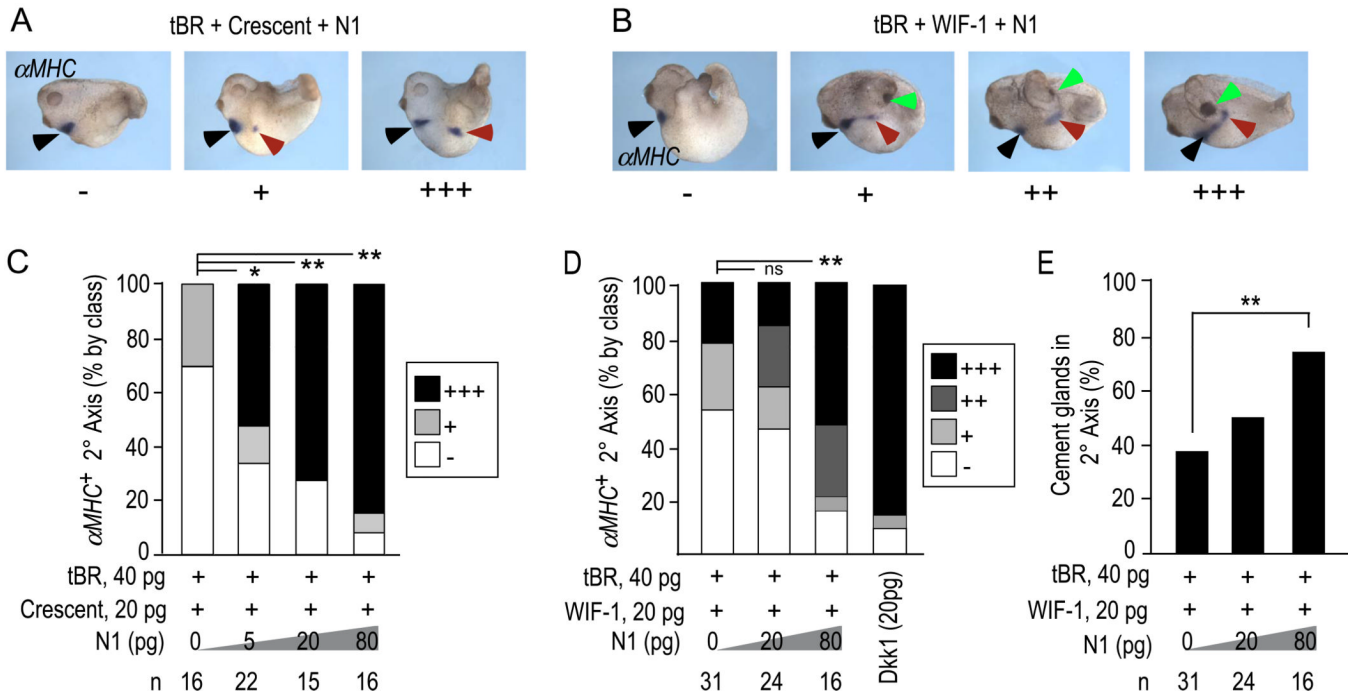

Figure 4. N1 synergizes with WIF-1 and Crescent to induce heart and cement gland

A, B) Examples of embryos as in Fig. 3 cultured to stage 28–30 and stained by in situ hybridization for α*MHC* to reveal developing myocardial tissue in primary (black arrow) and secondary (red arrow) body axes. N1 in conjunction with WIF-1, but not Crescent increased the incidence of cement glands (green arrows).

C, D) Quantification of the percentage of ectopic heart field induced in response to N1 plus Crescent (C) or WIF-1 (D), and according to class (+/−, +, ++, and +++) as in panels A and B. p-values were calculated by the Chi-square test [**, <0.001; *, <0.05; ns, not significant (>0.05)]. Results showing complementarity are for 20 pg of Crescent and WIF-1; similar outcomes were observed in additional experiments using 10 and 40 pg doses of both Crescent and WIF-1.

E) Quantification of the incidence of cement gland formation in response to WIF-1, N1 and tBR. N1 did not alter the lack of cement gland induction by Crescent and tBR (not shown, but see text). ** indicates p value <0.001 as calculated by Student's T-test.

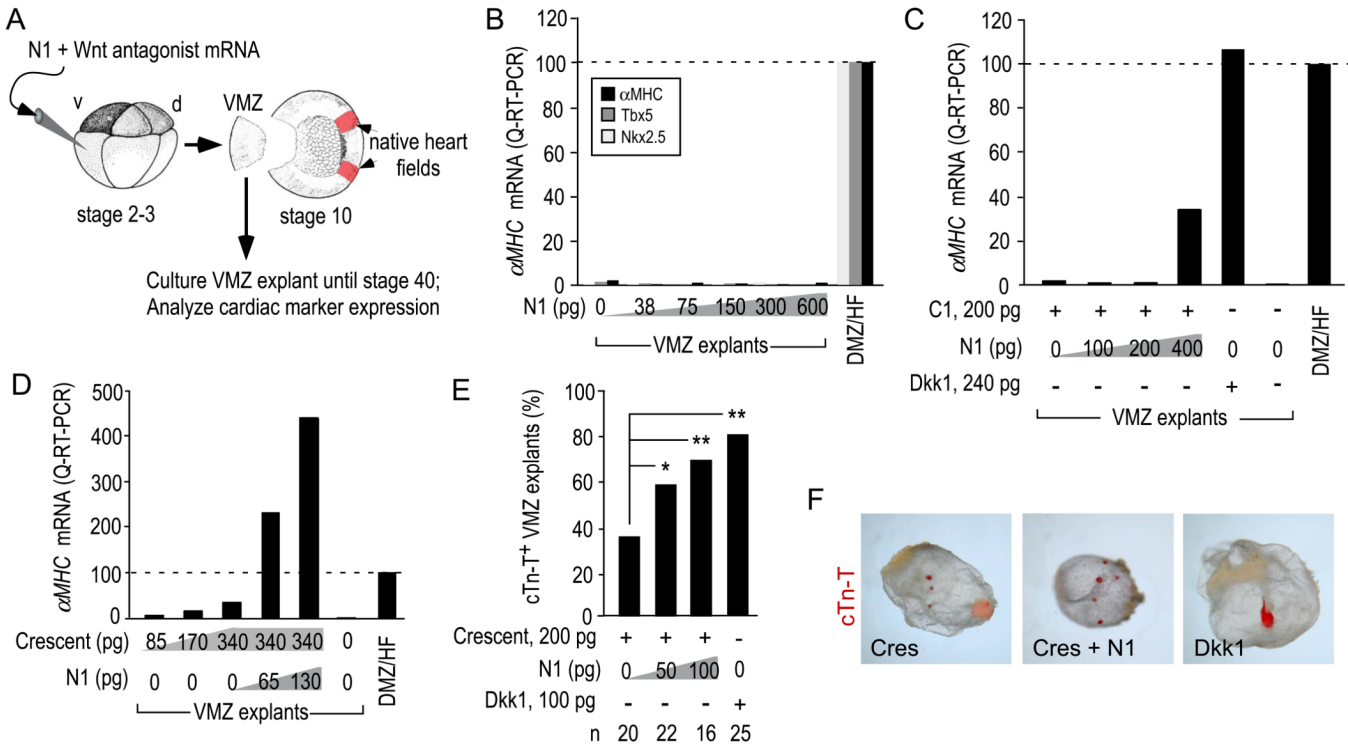

Figure 5. N1 synergizes with Wnt antagonists directly to induce heart tissue

A) Diagram of the VMZ explant assay. Isolated explants were cultured until stage 28 for analysis of *Nkx2.5* and *Tbx5* or stage 34 for α*MHC* expression by quantitative RT-PCR (B–D) or stage 40 for incidence of cTn-T^{+} explants by immunostaining (E,F).

B) N1 alone did not induce *Nkx2.5*, *Tbx5* or α*MHC* through a dose range of 38–600 pg of injected mRNA, whereas the native heart field (HF) in DMZ explants expressed each marker as expected.

C,D) The effect of N1 plus a constant amount of C1 (C) or Crescent (D) on α*MHC* induction. The experiments are representative examples of at least 3 trials.

E) Incidence of VMZ explants with ectopic cTn-T^{+} myocardial tissue. p-values were calculated by the Chi-square test [**, <0.001; *, <0.05].

F) Whole mount view of stage 40 VMZ explants immunostained with anti-cTn-T showing that although N1 increased the incidence of cTn-T^{+} explants, they retained the small, dispersed foci characteristic of Crescent-induced myocardial tissue. Fluorescent image (red) is superimposed on brightfield image of explant.

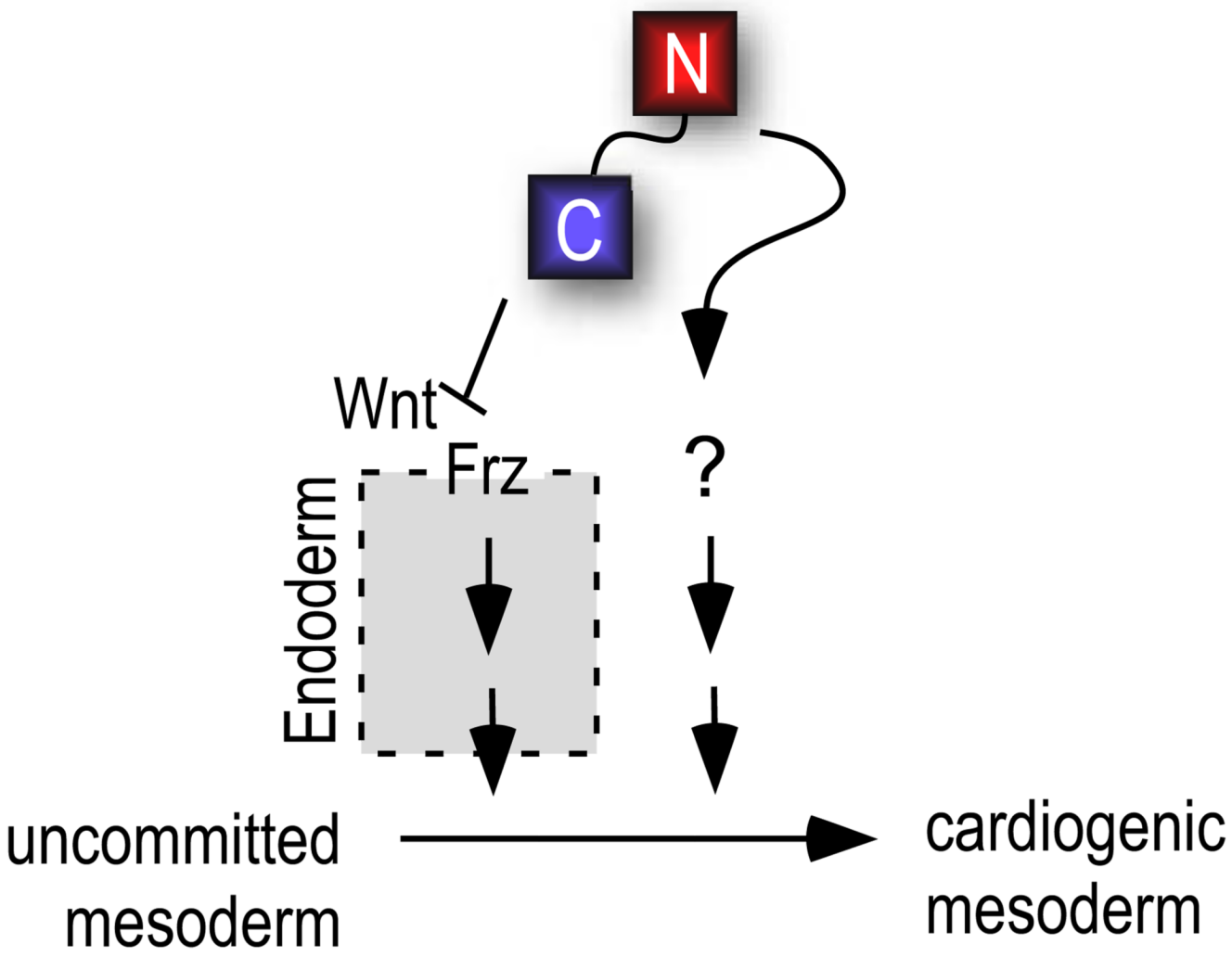

Figure 6. Model for independent function of N1 and C1 in heart induction

C1 acts indirectly by inhibiting Wnt signaling in the endoderm stimulate the production of a diffusible intermediary that initiates cardiogenesis in mesoderm (Foley and Mercola, 2005). N1 might act on endoderm or directly on cardiogenic mesoderm (see text).